



HAL
open science

How Accurately Can DFT Describe Non-valence Anions?

Guillaume Thiam, Franck Rabilloud

► **To cite this version:**

Guillaume Thiam, Franck Rabilloud. How Accurately Can DFT Describe Non-valence Anions?. *Journal of Chemical Theory and Computation*, 2023, 19 (10), pp.2842-2849. 10.1021/acs.jctc.3c00099 . hal-04156373

HAL Id: hal-04156373

<https://hal.science/hal-04156373>

Submitted on 8 Jul 2023

HAL is a multi-disciplinary open access archive for the deposit and dissemination of scientific research documents, whether they are published or not. The documents may come from teaching and research institutions in France or abroad, or from public or private research centers.

L'archive ouverte pluridisciplinaire **HAL**, est destinée au dépôt et à la diffusion de documents scientifiques de niveau recherche, publiés ou non, émanant des établissements d'enseignement et de recherche français ou étrangers, des laboratoires publics ou privés.

How accurately can DFT describe non-valence anions?

Guillaume Thiam* and Franck Rabilloud*

*Université de Lyon, Université Claude Bernard Lyon 1, CNRS, Institut Lumière Matière,
UMR5306, F-69622 Villeurbanne, France*

E-mail: guillaume.thiam@univ-lyon1.fr; franck.rabilloud@univ-lyon1.fr

Abstract

Weakly bound non-valence anions are molecular systems where the excess electron stabilizes in a very diffuse orbital whose size, shape, and binding energy ($\sim 1 - 100$ meV) are governed by the long-range electrostatic potential of the molecule. Its binding energy comes mainly from charge-dipole or charge-multipole interactions, or dispersion forces. While highly correlated methods, like coupled cluster methods, are considered to be the state of the art for describing anionic systems, especially when the electron lies in a very diffuse orbital, we consider here the possibility to use DFT-based calculations. In such molecular anions, the outer electron experiments long-range exchange and correlation interactions. We show that DFT can describe long-range bound states provided that a correct asymptotic exchange and correlation potential is used, namely, that from a range-separated hybrid functional. This opens an alternative to the computationally demanding highly correlated method calculations. It is also suggested that the study of weakly bound anions could help in the construction of new DFT potentials to study systems where non-local effects are significant.

1 Introduction

There is a substantial class of molecules that are able to bind an additional electron in a very delocalized and diffuse nonvalence orbital through long-range interactions, i.e. charge-multipole, polarization or dispersion interactions.¹ Such weakly bound anions (the binding energy is typically ~ 1 -100 meV) have been observed for a few tens of molecules. In the most frequently encountered cases, the molecule together with the additional electron form a so-called dipole-bound anion, where the electron is attached thanks to the electrostatic dipole potential of the molecule.²⁻⁸ It is well established that, in the Born-Oppenheimer approximation, a polar molecule possessing a dipole moment larger than a critical value, being of the order of 1.625 Debye, is able to bind an excess electron.⁹⁻¹¹ Dipole-bound states appeared as a class of doorway states to valence type states,¹² and in the case the valence state is dissociative, as a doorway to dissociative electron attachment processes.¹³

Quadrupole-bound anions^{14,15} where the electron is bound to the molecule via the charge-quadrupole interaction have also been observed.^{4,15} Finally, there also exist some long-distance bound states where the excess electron is bound by correlation effects, primarily dispersion and polarization.¹⁶⁻²¹ In such cases, the electron is unbound at the Hartree-Fock level, but, including correlation effects allows the excess electron to be bound. In dipole-bound anions, the electron is found away from the molecule on the positive end of the dipole, while in quadrupole- and correlation-bound anions, the electron usually lies around the molecule (see Figure 1). The average distance to the molecule is typically $> 10\text{\AA}$, contrary to their valence counterparts occupying compact orbitals.

Some works have shown that valence states and weakly bound states can be coupled, and their coupling constant has been calculated in some cases to be typically about ~ 10 -30 meV.^{12,22} Therefore, weakly bound anions could represent an intermediate step between continuum scattering states and stable or metastable valence states, being able to act as an aid in capturing thermal electrons.^{3,12,13,23} Henceforth, they are expected to play a significant role in electron-attachment phenomena.

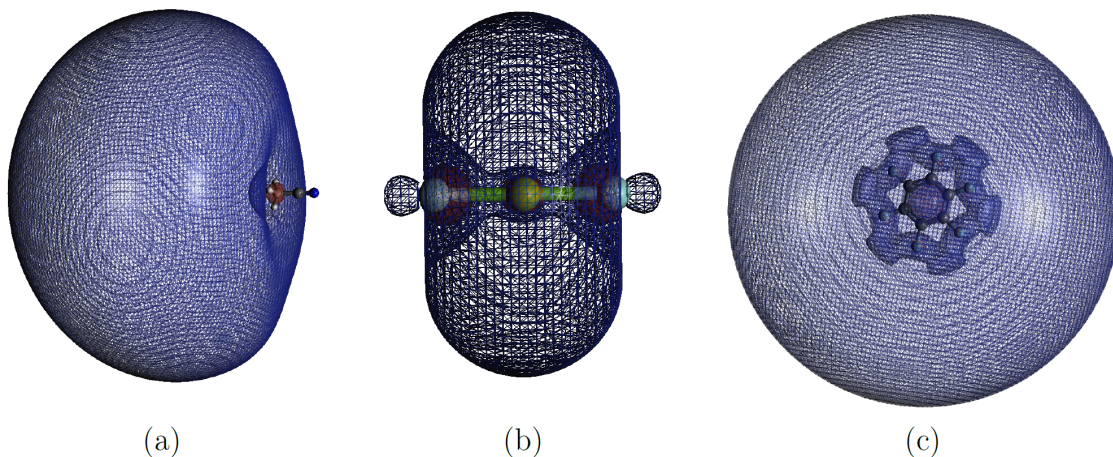


Figure 1: (a) Dipole-bound type orbital for the acetonitrile (CH_3CN) molecule. (b) Quadrupole-bound type orbital for the FMgF molecule. (c) Correlation-bound type orbital for the perfluorobenzene (C_6F_6) molecule. All surfaces shown encloses 50 % of the charge density.

1.1 Weakly bound anions from post-Hartree-Fock calculations

Computing electron binding energies associated with non-valence states is quite challenging and requires non-standard basis sets and electronic structure methods. Indeed, as weakly bound anions are characterized by the very diffuse orbital occupied by the excess electron and their very low electron binding energies, a very large basis set with extra diffuse functions is needed.^{11,19,21,24} Nevertheless, the mere use of very large basis sets is not sufficient to describe correctly the properties of weakly bound anions. While Hartree-Fock calculations combined with an extra large basis set might bind the additional electron in the case of a dipole-bound state, but usually with a significant underestimation of the binding energy, they are unable to bind the excess electron in the case of correlation-bound anions or quadrupole-bound anions. In such cases, the Hartree-Fock orbital of the excess electron will describe a neutral system plus an electron in a discretized continuum orbital.²⁵ Post-Hartree-Fock calculations, such as MP2 or CCSD(T) calculations, may encounter difficulties to converge toward a non-valence anion, particularly in the case of quadrupole-bound or correlation-bound anions. Nowadays, the state-of-the-art for describing weakly bound anions are EOM-CCSD and EA-EOM-CCSD methods²⁶ combined with the use of extra diffuse functions which can be

centered either on the atoms or on off-atom sites. These methods scale in n^6 with the number of orbital functions, then adding extra diffuse functions around all atoms would result in a drastic increase of the computational cost.²¹ Henceforth, these methods are limited to fairly small systems.

1.2 Weakly bound anions with DFT: the case of global hybrid functionals

A good alternative to post-Hartree-Fock methods, with far less computational costs, resides in the density-functional theory (DFT) calculations. If the latter are able to describe weakly bound anions, this could offer some perspectives to study larger systems. Generalized gradient approximation (GGA) functionals suffer from the self-interaction error and fail to describe the binding of a long-range anionic state. Commonly used global hybrid functionals are not suitable as well.²⁷⁻²⁹ In a prior work, Jensen²⁷ showed that local or hybrid global functionals calculate atomic anions as having only a fraction of the extra electron bound, i.e., a part of the electron density goes to infinity, and investigated the consequences of this failure in the description of intermolecular complexes or donor-acceptor systems. We report here some results performed using the functionals BHandHLYP³⁰ with 50% portion of Hartree-Fock exchange and B3LYP^{31,32} (19% of Hartree-Fock exchange) for a couple of molecules. We used an extended basis set, labeled (3sp)-aug-cc-pvtz in the next section, which includes several atom-centered extra-diffuse functions (see below for details about it). The calculated electron binding energy (eBE) is positive (Table 1). But, the plot of the radial distribution function (RDF) of the charge density associated with the additional electron reveals that the electron occupies a nonphysical state, since a significant part of the charge is very far at the end of the simulation box while only a part ($\sim 50\%$) of the charge density can be allocated to a bound state. In Figure 2, the RDF for the nitromethane molecule (CH_3NO_2) exhibits two well-separated hills at around 5 and 35 Å, the latter being due to the finiteness of the basis set. Consequently, the electron binding energy calculated with global hybrid

functionals should not be considered, since calculations describe a non-physical state where only a small part of the electron is bound to the molecule.

Table 1: Calculated eBE (in meV) with global hybrid functional B3LYP and BHandHLYP at (3sp)-aug-cc-pvtz level, compared with experimental data, except for FMgF and perfluorobenzene for which it is compared to EA-EOM-CCSD calculations.^{14,16}

molecule	B3LYP	BH&HLYP	Expt
Acetaldehyde	114.689	7.606	0.6 ^a
Acetone	131.613	13.355	2.8 ^b
Acetonitrile	-	47.022	19.3 ^a
FMgF	684.446	438.018	269 ^c (EA-EOM)
Nitromethane	160.540	42.087	12 ^d
Perfluorobenzene	-	98.414 (2sp)	135 ^e (EA-EOM)
Thymine	-	82.007	69 ^f

^aRef³³ ; ^bRef³⁴ ; ^c Ref¹⁴ ; ^d Ref² ; ^e Ref¹⁶ ;

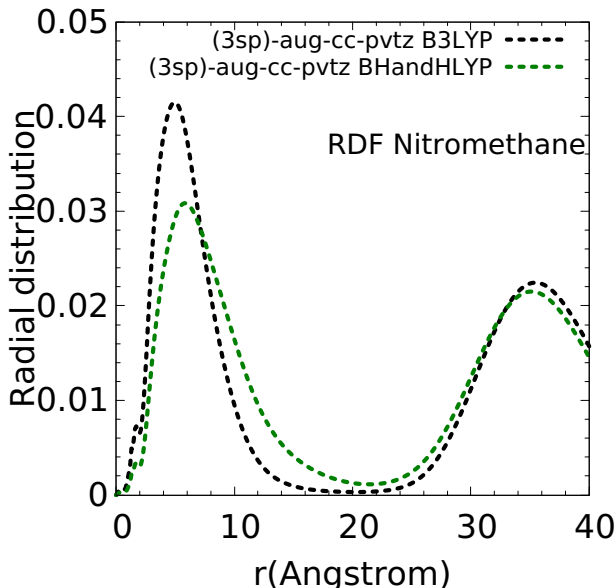


Figure 2: Radial Distribution Function (RDF) of the excess-electron density around nitromethane, calculated with global hybrid functionals BHandHLYP and B3LYP. The green or black dashed line corresponds to the RDF calculated with BHandHLYP or B3LYP functional, respectively.

The inability of global hybrids to correctly bind a charge lying at a long distance is

due to their incorrect asymptotic behavior.^{27,35} It was shown that the incorrect distance dependence of the exchange functional is responsible for this failure.²⁷ Several solutions have been proposed,^{27,35,36} among which is the use of long-range corrected hybrid functionals where the part of HF exchange increases continuously with the electron-electron distance. Recently, it was shown that such schemes are free of self-interaction errors when the range-separation parameter μ is chosen so that the DFT Koopmans’ theorem is satisfied for the anion.³⁵

When considering anions, the basis set should contain very diffuse functions.^{27,35,37} In previous works,^{27,35} DFT calculations were performed with basis sets containing extremely diffuse functions, the exponent of the most diffuse function was less than 10^{-10} . However, when using the range-separated hybrid functional with a tuned range-separated parameter, increasing the diffuseness of basis set with exponents less than $\sim 10^{-3}$ or $\sim 10^{-4}$ has a small effect on the electron affinities values.³⁵

2 Method

In order to treat weakly bound anions correctly, we choose to work with a range-separated hybrid (RSH) functional with 100% Hartree-Fock exchange at long range, namely the ω B97x³⁸ functional which contains an increasing amount of exact Hartree-Fock exchange, from 16% at the short range to 100% at the long range. This is one of the most efficient functional for a wide variety of excited state calculations.³⁹ It has also been used recently to tackle the calculation of resonant electron attachment energy and performed quite well.^{40–42}

We constructed a large basis set from the basis set aug-cc-pvtz⁴³ and completed it by adding extra diffuse functions with s and p symmetries. The additional exponents were obtained by multiplying the previous most diffuse exponent by 0.3 as suggested in previous works.^{44,45} The present constructed basis sets are called (Nsp)-aug-cc-pvtz where N stands for the number of s and p functions added. In the following, (0sp)-aug-cc-pvtz will refer to the

aug-cc-pvtz basis set. It is important to emphasize that converging the calculation toward a proper weakly bound anionic state with such large basis sets is sometimes troublesome due to a competition with the discrete continuum states. Therefore, calculations sometimes required starting from a previous one performed with a smaller basis set and converged in a weakly bound type orbital and not in a discrete continuum one.

All DFT calculations were performed with the Gaussian16 suite of programs.⁴⁶ All geometries were optimized at the ω B97x/aug-cc-pvtz level. Pre- and post-processing operations are performed using the graphical interface Gabedit.⁴⁷ The radial distribution functions (RDF) were plotted using the Multiwfn software.⁴⁸

3 Results

We have considered a large sample of molecules (see Figure SI1). It is composed of molecules studied by Abdoul-Carime and Desfrancois⁴ who succeeded in measuring the eBE and proposed a simple electrostatic model including the contributions from the dipolar, quadrupolar and polarization forces to evaluate eBEs. The sample was enlarged with other types of systems, such as correlation-bound or quadrupole-bound anions.

The dipole moment and isotropic polarizability have been computed using (0,1,2,3 and 4sp)-aug-cc-pvtz basis sets. The values obtained for dipole-moment and isotropic polarizability remain constant with the size of the basis set (see tables SI1 and SI2). They are in agreement with the available experimental data. Calculated dipole moments are usually around 0.3 D from the experimental values, except for pivaldehyde where the calculated value overestimates by ~ 0.9 D the experimental one. Regarding the isotropic polarizabilities, the calculated values are very near to experimental data. So, the overall description of electrostatic properties such as dipole-moment or polarizabilities is quite accurate.

Table 2: Calculated electron binding energies (eBEs), in meV, compared to experimental data (Rydberg Electron Transfer experiments mainly) and EA-EOM-CCSD calculations. (Nsp) means aug-cc-pvtz with N additional *s* and *p* functions.

molecule	present work					references	
	(0sp)	(1sp)	(2sp)	(3sp)	(4sp)	Expt	EA-EOM-CCSD
Acetaldehyde	-649.392	-114.52	2.245	19.513	21.374	0.6 ^a	
Acetone	-626.577	-110.503	4.031	20.844	22.893	2.8 ^b	2.1 ^{b,o}
Acetonitrile	-508.439	-68.772	18.158	30.596	30.481	19.3 ^a	12.8 ^{m,o}
Adenine	-454.793	-92.701	5.294	20.647	21.126	11.5 ^d	
Benzonitrile	-202.484	-58.267	24.946	33.339	33.423	28 ^d	24 ⁿ
Butanal	-619.680	-102.054	8.044	20.592	24.699	1.2 ^a	
Cyclopentanone	-628.357	-95.832	9.105	23.924	25.632	2.8 ^a	
FMgF	109.834	140.124	142.973	143.021	143.029		269 ^e
NaONa	-71.283	-16.821	-	-	-		29.7 ^e
Nitromethane	-541.351	-78.205	13.719	26.598	27.230	12 ^f	13 ^l
Perfluorobenzene	-612.589	-36.622	15.089	-	-		135 ^g
Pivaldehyde	-637.77	-115.869	2.101	21.206	23.377	1 ^d	
Pyridazine	-483.768	-61.099	19.171	31.273	31.321	20 ^d	19 ^j
Succinonitrile (gauche conformer)	-234.005	41.356	73.328	74.235	74.234	108 ^h	127 ^e
Thymine	-333.912	-24.752	33.263	38.118	38.116	69 ⁱ	51 ^{k,o}

^a Ref³³ ; ^bRef³⁴ ; ^c Ref⁴⁹ ; ^d Ref⁴ ; ^e Ref¹⁴ ; ^f Ref⁶ ; ^g Ref¹⁶ ; ^h Ref;^{15,50} ⁱ Ref⁵¹ ; ^j Ref⁵² ; ^k Ref⁵³ ; ^l Ref⁵⁴ ; ^m Ref⁵⁵ ; ⁿ Ref⁵⁶ ; ^o CCSD/MP2 or CCSD(T) calculation.

Calculated eBE can be found in Table 2, together with the available experimental data and estimation from coupled cluster calculations, most often at EA-EOM-CCSD level. At (0sp)- and (1sp)-aug-cc-pvtz levels, the electron is unbound, therefore, these basis sets are not adapted to treat these systems. Actually, the electron is confined in a too-small box. To illustrate that, we plot in Figure 3 the RDF of the orbital occupied by the excess electron around the acetone molecule for all considered basis sets. In the case of (0sp) and (1sp)-aug-cc-pvtz, though the orbitals are dipole-bound like, the electron still remains too close to the molecule for the system to stabilize the electron. Also, the (2sp)-aug-cc-pvtz basis set keeps the excess electron too close to the molecule while larger basis sets stabilize the electron further away. The plotted RDF with (3,4)-aug-cc-pvtz basis set are quite similar and exhibit the expected behavior: a diffuse orbital (hill around ~ 20 Å) corresponding to a bound state. For completeness, the RDF for other molecules (acetaldehyde, acetonitrile, pyridazine and thymine) are given in Figure SI2.

In Table 2, the (2sp)-aug-cc-pvtz is the smallest basis set in our selection that allows the

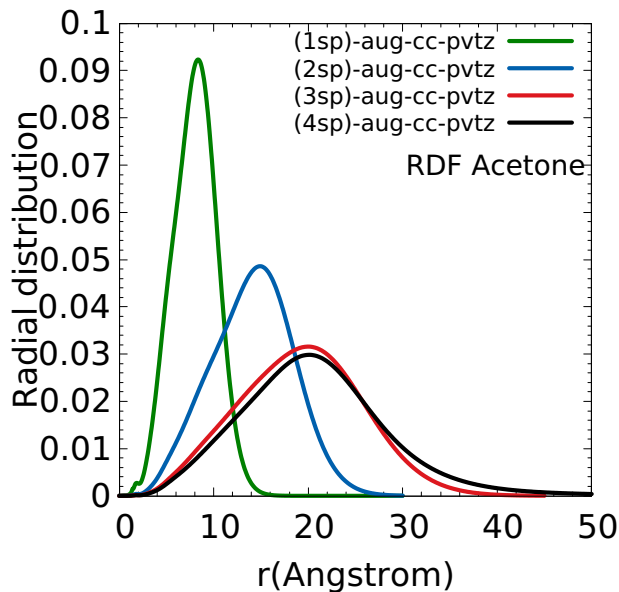


Figure 3: Radial distribution function of the electron around the Acetone molecule calculated with ω B97x functional and (1 [green],2 [blue],3 [red],4 [black]sp)-aug-cc-pvtz basis sets.

molecules to bind the additional electron. eBE does not vary significantly when calculated with (3sp)- or (4sp)-aug-cc-pvtz. In order to find the most appropriate basis set, we have calculated the eBE to the nitromethane molecule using gradual extensive basis sets. First, we generated intermediate basis sets between (1sp) and (2sp): to (1sp)-aug-cc-pvtz, we added one s and p functions whose exponents were obtained by multiplying the previous most diffuse exponents by successively 0.9, 0.8, 0.7, 0.6, 0.5, 0.4, 0.3 (the multiplication of 0.3 gives (2sp)-aug-cc-pvtz). Similar processes were made starting from (2sp) and (3sp) until reaching (4sp)-aug-cc-pvtz. The curve representing the nitromethane eBE with respect to the spatial extent is plotted in Figure 4. This curve exhibits an optimal value with the (3sp)-aug-cc-pvtz basis set augmented with one additional s and p functions whose exponents were determined by multiplying by 0.8 the previous ones. However, we notice that the eBE does not vary a lot between (3sp) or (4sp)-aug-cc-pvtz basis set (~ 2 meV in the least favorable case for the acetone molecule, see Table 2). Therefore, we have chosen to consider the results obtained with the (3sp)-aug-cc-pvtz basis set. Overall, the agreement between the calculated

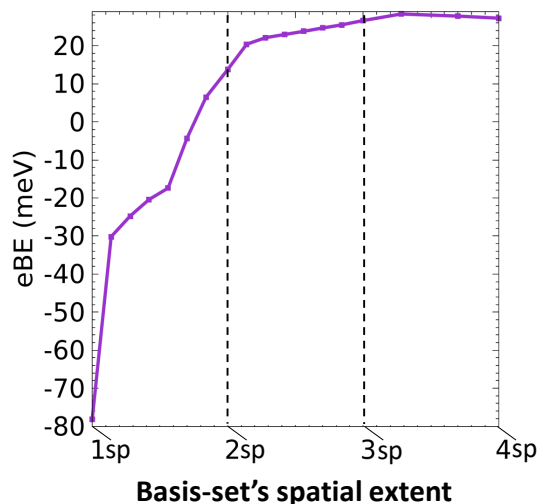


Figure 4: Evolution of the electron binding energy with respect to the size and the spatial extent of the basis set.

eBE with (3,4sp)-aug-cc-pvtz basis set, and the experimental data or EA-EOM-CCSD values remains satisfying. The root-mean-square deviation from experimental values is calculated to be 19.52 meV. The least favorable case is with the succinonitrile where the calculated value is 33.8 meV lower than the experimental value. The most favorable case is the benzonitrile where the calculated value is 5.3 meV above the experimental value. Interestingly, the increasing value of eBE with the value of the dipole moment μ of the molecule is reproduced in our calculations. The relationship between eBE and μ is highlighted in figure SI3.

In most cases, the calculated eBE value overestimates the experimental one, the exceptions being: FMgF, NaONa, perfluorobenzene, succinonitrile and thymine. Perfluorobenzene is expected to form a correlation-bound anion, FMgF and NaONa are quadrupole-bound anions, while the contribution of quadrupole and polarization terms are expected to be important for succinonitrile and thymine.¹⁴ For the five molecules, correlation is likely to be an important contribution. For succinonitrile and thymine, the calculated eBE (74 and 38 meV) underestimates the experimental one by ~ 30 meV, while the Coupled Cluster values were calculated to be 127 and 51 meV (Table 2). For FMgF, NaONa and perfluorobenzene,

it is only possible to compare with previous EA-EOM-CCSD calculations that are expected to be quite accurate.^{14,16} For FMgF, our calculated value is about 120 meV smaller than the EA-EOM-CCSD value calculated by Sommerfeld.¹⁴ For NaONa, we are unable to converge toward a weakly bound state with basis sets larger than (1sp)-aug-cc-pvtz. For the perfluorobenzene, we are unable to converge toward a weakly bound state with basis sets larger than (2sp)-aug-cc-pvtz, i.e., calculation converges toward a continuum state. The reason may be a somewhat insufficiently good description of correlation. This point will be detailed below.

Lastly, we also compared the RDF we calculated for the FMgF molecule to the density of the excess electron calculated by Sommerfeld at the EA-EOM-CCSD level in ref.¹⁴ Both curves are quite similar (see Figure 5), suggesting that RSH-DFT could provide RDF competing with the ones calculated with post-Hartree-Fock methods.

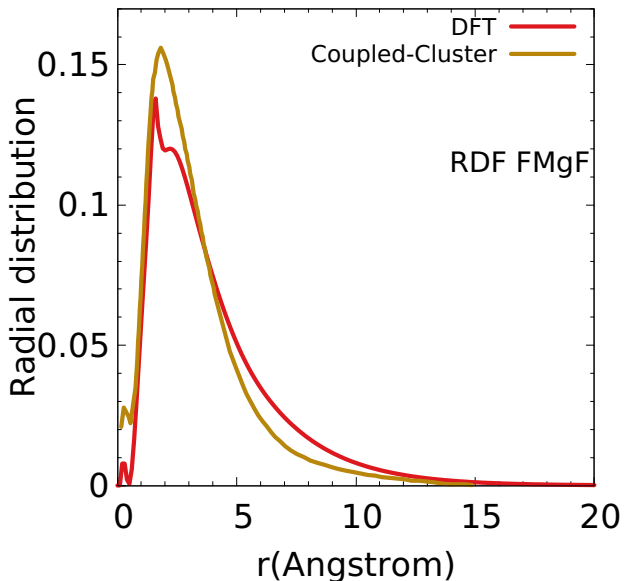


Figure 5: Radial distribution function (in a.u.) of the excess electron density for FMgF calculated at the DFT ω B97x/(3sp)-aug-cc-pvtz level compared to that¹⁴ obtained at Coupled Cluster (EA-EOM-CCSD) level.

Therefore, DFT calculations with RSH functional are able to describe weakly bound anions. eBEs are calculated with a precision of about ~ 0.02 eV in the case of dipole-

bound states, and the RDF description does not exhibit the flaws obtained with global hybrid functionals. The present DFT calculations are not as accurate as EA-EOM-CCSD calculations (Table 2), but they furnish qualitative results on the prediction of the long-range anionic states.

4 Further development

In order to achieve a better agreement between the calculated eBE and the experimental values and also be able to bind the excess electron on systems like NaONa or perfluorobenzene, there are issues to be addressed.

4.1 Optimization of the range-separation parameter

Due to an excessive convexity of the exchange-correlation potential, the latter tends to go to zero slightly too rapidly. To correct this flaw, it is possible to refine the range-separation parameter ω .⁵⁷⁻⁶⁰ To do so, the range-separation parameter, ω , can be chosen so that the energy of the HOMO is equal to the opposite of the ionization potential:^{35,57,60}

$$\text{IP}(\omega) = -\epsilon_{\text{HOMO}}(\omega). \tag{1}$$

Since the calculated eBE are of the order of ~ 1 -100 meV, a small change in the exchange-correlation potential could play a significant role in the evaluation of the eBE. For a couple of systems, we looked for the optimal value for ω such that equation (1) was satisfied up to 10^{-1} eV (see Table 3). However, the calculated eBE were not significantly affected, the largest change occurring for the nitromethane where the difference is of 1.12 meV.

Table 3: eBE values (in meV) calculated with the optimized or default value of ω , corresponding ionization potential (IP) in eV, HOMO’s energy in eV. The default value of ω is 0.3 Bohr^{-1} .

molecule	$\omega \text{ (Bohr}^{-1}\text{)}$	IP(ω) (eV)	$\epsilon_{HOMO}(\omega)$ (eV)	eBE _{optimized} (meV)	eBE _{default} (meV)
Acetaldehyde	0.32	10.20	-10.14	19.61	19.51
Acetonitrile	0.35	12.33	-12.30	30.75	30.60
Acetone	0.30	9.66	-9.70	20.84	20.84
FMgF	0.43	13.99	-13.91	143.62	143.02
Nitromethane	0.36	11.84	-11.77	27.72	26.60
Pyridazine	0.27	9.07	-9.13	31.13	31.27

To investigate further the influence of ω , we tried varying ω from 0.1 to 1.0 Bohr^{-1} , but the change in the calculated eBEs was up to $\sim 3\text{-}6 \text{ meV}$ in the most extreme cases. Results for acetaldehyde and nitromethane can be found in Figure 6. Therefore, we think that the

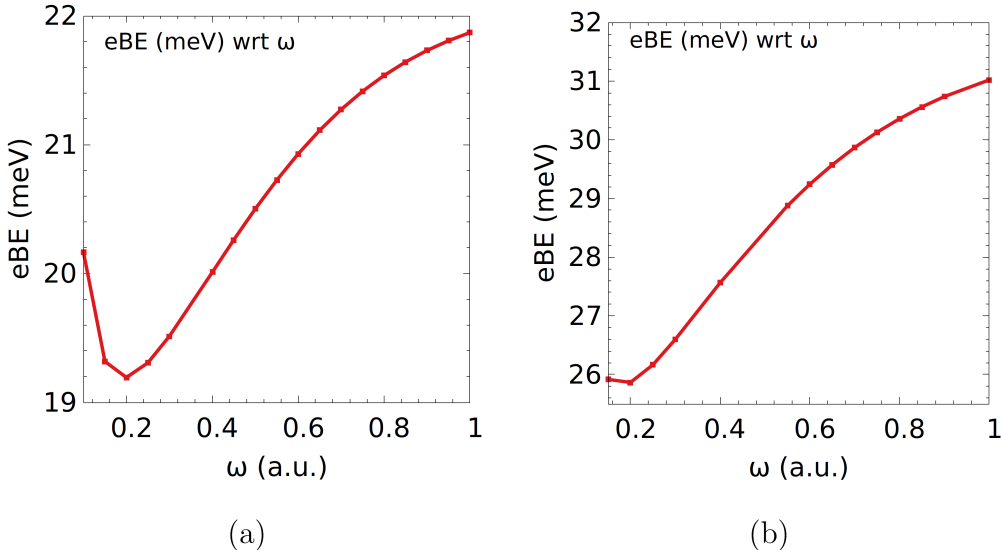


Figure 6: Calculated eBE using (3sp)-aug-cc-pvtz basis set, with respect to range-separation parameter ω for the (a) acetaldehyde and (b) nitromethane.

range-separation parameter optimization is not what primarily causes the overestimation of eBEs.

4.2 The influence of the correlation

Since correlation is expected to play an important role for weakly bound anions, we tried using double-hybrid functionals. Namely, we used PBEQIDH⁶¹ built as a global hybrid,

including 70 % of exact Hartree-Fock exchange while the correlation part contains 33 % of Møller-Plesset perturbation (MP2) contribution. Due to its global hybrid character, PBE-QIDH is not expected to perform better than ω B97x, but it can inform us on the role of the correlation by analyzing the importance of the MP2 contribution to the eBE. To do so, we calculated:

$$\Delta E_2 = E_2(\text{Neutral}) - E_2(\text{Anion}), \quad (2)$$

where $E_2(\text{Neutral})$ and $E_2(\text{Anion})$ are the MP2 energy correction for the molecule and anion respectively. These energies are accessible in Table 4. Overall regarding the eBEs, as ex- Table 4: Calculated eBE values at PBEQIDH/(3sp)-aug-cc-pvtz level, together with the ΔE_2 contribution to eBE. Energies in meV.

molecule	ΔE_2	eBE
Acetaldehyde	0.46	33.088
Acetone	2.04	34.821
Acetonitrile	5.34	60.130
FMgF	80.88	339.976
Nitromethane	1.2	51.646
Perflurobenzene	18.40	44.159
Thymine	12.00	90.923

pected, PBEQIDH does not perform better than ω B97x. In most cases, the overestimation of the eBE is more important. The exceptions being thymine, FMgF, and perflurobenzene where the eBE evaluation gives values that are closer to the expected values for thymine and FMgF, and allowed to bind the excess electron in a correlation-bound state for the perflurobenzene at the (3sp)-aug-cc-pvtz level, even though the calculated eBE is still smaller than the one calculated by Jordan et al. at EA-EOM-CCSD level¹⁶ (44 vs 135 meV, Table 2). The biggest MP2 contribution to the eBE are obtained for FMgF, perflurobenzene and thymine with values of 80, 18 and 12 meV respectively. Adding ΔE_2 to the eBE obtained with ω B97x (values in Table 2) for the thymine molecule or FMgF gives corrected eBEs of about ~ 50 meV for thymine and ~ 224 meV for FMgF, which is much closer to reference values (respectively 69 meV and 269 meV). Even though the density used to

evaluate the MP2 correction is not the same as the one obtained with ω B97x, this gives interesting information about the potentially missing correlation energy with ω B97x. Additionally, for systems such as acetaldehyde, acetonitrile, acetone, nitromethane, where the electron mainly interacts via dipole-charge forces, the MP2 contribution is relatively small compared to the calculated energy. It is noteworthy that PBEQIDH, contrary to standard global hybrid functionals, is able to bind the excess electron, even at a large distance, and in spite of its global hybrid character regarding exchange. The plot of the RDF shows that PBEQIDH tends to stabilize the electron a little closer to the molecule than ω B97x does, except in the case of FMgF for which both functionals perform similarly (Figure SI4).

In view of our results, it seems likely that the addition of an MP2 correction to RSH functionals could increase the eBE for quadrupole or correlation-bound systems, without increasing the eBE of dipole-bound systems. A further development would be to use range-separated double hybrid functionals which decompose the electron-electron interaction for both exchange (RSH scheme) and correlation, the latter combining the DFT correlation potential with MP2, coupled Cluster, or random-phase approximations.^{62,63} Furthermore, the addition of such a correction might stabilize the excess electron slightly closer to the molecule for dipole-bound systems, which could give eBE smaller than those calculated with ω B97x and therefore give predictions closer to the experimental values. For quadrupole- or correlation-bound systems, this might facilitate the stabilization of the excess electron and could allow describing systems like perfluorobenzene or NaONa that were inaccessible to ω B97x.

5 Conclusions

To conclude, DFT calculations with RSH functionals are able to describe weakly bound anions, particularly in the case of dipole-bound states. The spatial extent of the orbital occupied by the excess electron corresponds to a long-distance bound state, as expected. The

predictions of the electron binding energies slightly overestimate the experimental values, except in the case of correlation-bound anions, for which a significant failure is observed. Some possible improvements, based on calculations performed with double-hybrid functionals, have been proposed. They suggest using range-separated double hybrid functionals to better evaluate the dispersion part.

Lastly, studying weakly bound anions in the DFT framework allows exploring the most fundamental aspects of the theory, as states yield highly non-local effects and very low energies. Reference data is available from experiments or from highly correlated methods calculations. And, this could help to build new potentials adapted to long-range bound states, which could be then used in other areas where non-local effects are also significant.

Acknowledgement

The authors thank Dr. Hassan Abdoul-Carime for introducing them to the fascinating topic of dipole-bound anions.

This work was performed using HPC resources from GENCI-IDRIS (Grant A0130807662) and the Pôle Scientifique de Modélisation Numérique (PSMN). It has received a financial support from the French National Research Agency (ANR-PRC BAMBI grant number 18-CE30-0009-03).

Supporting Information Available

Calculated dipole moment compared to experimental data, Calculated isotropic polarizability compared to experimental data, Structures of the studied molecules, Radial distribution function calculated at ω B97x/(2,3,4sp)-aug-cc-pvtz level for acetaldehyde, acetonitrile, pyridazine and thymine, Relationship between the electron binding energy (eBE) and the dipole moment of the molecule, RDF calculated at the PBEQIDH and ω B97x levels for acetaldehyde, acetone, acetonitrile, FMgF, nitromethane, thymine, The material is available free of

charge via the Internet at <http://pubs.acs.org>.

References

- (1) Simons, J. Molecular Anions. *J. Phys. Chem. A* **2008**, *112*, 6401–6511.
- (2) Desfrancois, C.; Abdoul-Carime, H.; Khelifa, N.; Schermann, J. P. From $\frac{1}{r}$ to $\frac{1}{r^2}$ Potentials: Electron Exchange between Rydberg Atoms and Polar Molecules. *Phys. Rev. Lett.* **1994**, *73*, 2436.
- (3) Compton, R.; Carman Jr., H.; Desfrancois, C.; H.Abdoul-Carime,; Schermann, J.; Hendricks, J.; Lyapustina, S.; Bowen, K. On the binding of electrons to nitromethane: Dipole and valence bound anions. *J. Chem. Phys.* **1996**, *105*, 3472.
- (4) Abdoul-Carime, H.; Desfrancois, C. Electrons weakly bound to molecules by dipolar, quadrupolar or polarization forces. *Eur. Phys. J. D* **1998**, *2*, 149–156.
- (5) Ard, . G.; Compton, R. N.; Garrett, W. R. Rotational auto-detachment of dipole-bound anions. *Chem. Phys. Lett.* **2016**, *650*, 154–158.
- (6) Liu, G.; Ciborowski, S. M.; Graham, J.; Buytendyk, A.; Bowen, K. Photoelectron spectroscopic study of dipole-bound and valence-bound nitromethane anions formed by Rydberg electron transfer. *J. Chem. Phys.* **2020**, *153*, 044307.
- (7) Castellani, M. E.; Anstöter, C. S.; Verlet, J. R. R. On the stability of a dipole-bound state in the presence of a molecule. *Phys. Chem. Chem. Phys.* **2019**, *21*, 24286.
- (8) Kang, D. H.; An, S.; Kim, A. K. Real-Time Autodetachment Dynamics of Vibrational Feshbach Resonances in a Dipole-Bound State. *Phys. Rev. Lett.* **2020**, *125*, 093001.
- (9) Fermi, E.; Teller, E. The capture of negative mesotrons in matter. *Phys. Rev.* **1947**, *72*, 399.

- (10) Turner, J. E. Minimum dipole moment required to bind an electron—molecular theorists rediscover phenomenon mentioned in Fermi-Teller paper twenty years earlier. *Amer. J. Phys.* **1977**, *45*, 758.
- (11) Jordan, K. D.; Wang, F. Theory of Dipole-bound Anions. *Annu. Rev. Phys. Chem.* **2003**, *54*, 367.
- (12) Sommerfeld, T. Coupling between dipole-bound and valence states: the nitromethane anion. *Phys. Chem. Chem. Phys.* **2002**, *4*, 2511–2516.
- (13) Sommerfeld, T. Dipole-bound states as doorways in (dissociative) electron attachment. *J. Phys.: Conf. Ser.* **2005**, *4*, 245.
- (14) Sommerfeld, T.; Dreux, K.; Joshi, R. Excess Electrons Bound to Molecular Systems with a Vanishing Dipole but Large Molecular Quadrupole. *J. Phys. Chem. A* **2014**, *118*, 7320–7329.
- (15) Liu, G.; Ciborowski, S. M.; Graham, J. D.; Buytendyk, A. M.; ; Bowen, K. H. The ground state, quadrupole-bound anion of succinonitrile revisited. *J. Chem. Phys.* **2019**, *151*, 101101.
- (16) Voora, V. K.; Jordan, K. D. Nonvalence Correlation-Bound Anion State of C_6F_6 : Doorway to Low-Energy Electron Capture. *J. Phys. Chem. A* **2014**, *118*, 7201–7205.
- (17) Rogers, J. P.; Cate, S. A.; Verlet, J. R. R. Ultrafast dynamics of low-energy electron attachment via a non-valence correlation-bound state. *Nature Chem.* **2018**, *10*, 341.
- (18) Rogers, J. P.; Cate, S. A.; Verlet, J. R. R. Evidence of Electron Capture of an Outgoing Photoelectron Wave by a Nonvalence State in $(C_6F_6)_n^-$. *J. Phys. Chem. Lett.* **2018**, *9*, 2504.
- (19) Sommerfeld, T.; Bhattarai, B.; Vysotskiy, V. P.; Cederbaum, L. S. Correlation-bound anions of NaCl clusters. *J. Chem. Phys.* **2010**, *133*, 114301–114308.

- (20) Bezchastnov, V. G.; Vysotskiy, V. P.; Cederbaum, L. S. Anions of Xenon Clusters Bound by Long-Range Electron Correlations. *Phys. Rev. Lett.* **2011**, *107*, 133401.
- (21) Voora, V. K.; Cederbaum, L. S.; Jordan, K. D. Existence of a Correlation Bound s-Type Anion State of C₆₀. *J. Phys. Chem. Lett.* **2013**, *4*, 849–853.
- (22) Tripathi, D.; Dutta, A. K. Electron Attachment to DNA Base Pairs: An Interplay of Dipole- and Valence-Bound States. *J. Phys. Chem. A* **2019**, *123*, 10131–10138.
- (23) Narayanan, J.; Tripathi, D.; Dutta, A. K. Doorway Mechanism for Electron Attachment Induced DNA Strand Breaks. *J. Phys. Chem. Lett.* **2021**, *12*, 10380–10387.
- (24) Gutsev, G. L.; Adamowicz, L. Electronic and geometrical structure of dipole-bound anions formed by polar molecules. *J. Phys. Chem.* **1995**, *99*, 13412–13421.
- (25) Voora, V. K.; Kairalapova, A.; Sommerfeld, T.; Jordan, K. D. Theoretical approaches for treating non-valence correlation-bound anions. *The Journal of Chemical Physics* **2017**, *147*, 214114.
- (26) Nooijen, M.; Bartlett, R. J. Equation of motion coupled cluster method for electron attachment. *J. Chem. Phys.* **1995**, *102*, 3629.
- (27) Jensen, F. Describing Anions by Density Functional Theory: Fractional Electron Affinity. *J. Chem. Theory Comput.* **2010**, *6*, 2726–2735.
- (28) Galbraith, J. M.; III, H. F. S. Concerning the applicability of density functional methods to atomic and molecular negative ions. *J. Chem. Phys.* **1996**, *105*, 862.
- (29) Rösch, N.; Trickey, S. B. Comment on "Concerning the applicability of density functional methods to atomic and molecular negative ions". *J. Chem. Phys.* **1997**, *106*, 8940–8941.
- (30) Becke, A. D. A new mixing of Hartree–Fock and local density-functional theories. *The Journal of Chemical Physics* **1993**, *98*, 1372–1377.

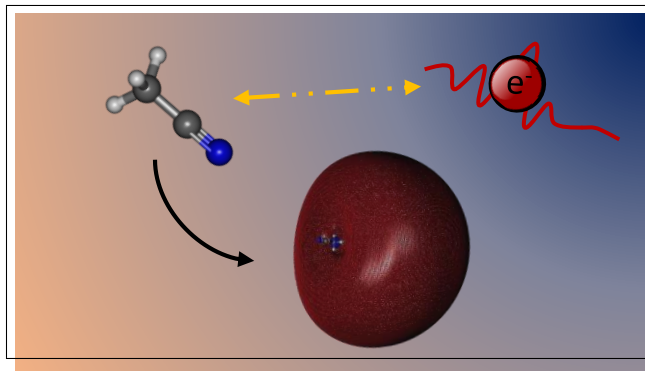
- (31) Becke, A. D. Density-functional thermochemistry. III. The role of exact exchange. *J. Chem. Phys.* **1993**, *98*, 5648–5652.
- (32) Stephens, P. J.; Devlin, F. J.; Chabalowski, C. F.; Frisch, M. J. Ab Initio Calculation of Vibrational Absorption and Circular Dichroism Spectra Using Density Functional Force Fields. *The Journal of Physical Chemistry* **1994**, *98*, 11623–11627.
- (33) Hammer, N. I.; Diri, K.; D., K.; Desfrancois, C.; Compton, R. N. Dipole-bound anions of carbonyl, nitrile, and sulfoxide containing molecules. *J. Chem. Phys.* **2003**, *119*, 3650–3660.
- (34) Hammer, N. I.; Compton, R. N. Isotope Effects in Dipole-Bound Anions of Acetone. *Phys. Rev. Lett.* **2005**, *94*, 153004.
- (35) Anderson, L. N.; Oviedo, M. B.; Wong, B. Accurate Electron Affinities and Orbital Energies of Anions from a Nonempirically Tuned Range-Separated Density Functional Theory Approach. *J. Chem. Theory Comput.* **2017**, *13*, 1656–1666.
- (36) Zhang, Y.; Weber, P. M.; Jónsson, H. Self-Interaction Corrected Functional Calculations of a Dipole-Bound Molecular Anion. *J. Phys. Chem. Lett.* **2016**, *7*, 2068–2073.
- (37) Jensen, F. Polarization consistent basis sets. III. The importance of diffuse functions. *J. Chem. Phys.* **2002**, *117*, 9234–9240.
- (38) Chai, J.; Head-Gordon, M. Systematic optimization of long-range corrected hybrid density functionals. *J. Chem. Phys.* **2008**, *128*, 084106.
- (39) Rabilloud, F. Description of plasmon-like band in silver clusters: The importance of the long-range Hartree-Fock exchange in time-dependent density-functional theory simulations. *The Journal of Chemical Physics* **2014**, *141*, 144302.
- (40) Thiam, G.; Rabilloud, F. Multi-Basis-Set (TD-)DFT Methods for Predicting Electron Attachment Energies. *J. Phys. Chem. Lett.* **2021**, *12*, 9995–10001.

- (41) Abdoul-Carime, H.; Thiam, G.; Rabilloud, F.; Charlieux, F.; Kopyra, J. Chemistry in Acetonitrile–Water Films Induced by Slow (<15 eV) Electrons: Application to the Earth and Space Chemistry. *ACS Earth and Space Chemistry* **2022**, *6*, 1126–1132.
- (42) Kopyra, J.; Wierzbicka, P.; Thiam, G.; Bald, I.; Rabilloud, F.; Abdoul-Carime, H. Experimental and theoretical studies of dissociative electron attachment to metabolites oxaloacetic and citric acids. *Int. J. Molecular Sciences* **2022**, *22*, 7676.
- (43) Kendall, R. A.; Dunning Jr., T. H.; Harrison, R. J. Electron affinities of the first-row atoms revisited. Systematic basis sets and wave functions. *J. Chem. Phys.* **1992**, *96*, 6796–6806.
- (44) Haiduke, R. L. A.; Bartlett, R. J. Can excitation energies be obtained from orbital energies in a correlated orbital theory? *J. Chem. Phys.* **2018**, *149*, 131101.
- (45) Hirao, K.; Chan, B.; Song, J.-W.; Bhattarai, K.; Tewary, S. Excitation energies expressed as orbital energies of Kohn–Sham density functional theory with long-range corrected functionals. *J. Comp. Chem.* **2020**, *41*, 1368–1383.
- (46) Frisch, M. J.; Trucks, G. W.; Schlegel, H. B.; Scuseria, G. E.; Robb, M. A.; Cheeseman, J. R.; Scalmani, G.; Barone, V.; Petersson, G. A.; Nakatsuji, H.; Li, X.; Caricato, M.; Marenich, A. V.; Bloino, J.; Janesko, B. G.; Gomperts, R.; Mennucci, B.; Hratchian, H. P.; Ortiz, J. V.; Izmaylov, A. F.; Sonnenberg, J. L.; Williams-Young, D.; Ding, F.; Lipparini, F.; Egidi, F.; Goings, J.; Peng, B.; Petrone, A.; Henderson, T.; Ranasinghe, D.; Zakrzewski, V. G.; Gao, J.; Rega, N.; Zheng, G.; Liang, W.; Hada, M.; Ehara, M.; Toyota, K.; Fukuda, R.; Hasegawa, J.; Ishida, M.; Nakajima, T.; Honda, Y.; Kitao, O.; Nakai, H.; Vreven, T.; Throssell, K.; Montgomery Jr., J. A.; Peralta, J. E.; Ogliaro, F.; Bearpark, M. J.; Heyd, J. J.; Brothers, E. N.; Kudin, K. N.; Staroverov, V. N.; Keith, T. A.; Kobayashi, R.; Normand, J.; Raghavachari, K.; Rendell, A. P.; Burant, J. C.; Iyengar, S. S.; Tomasi, J.; Cossi, M.; Millam, J. M.; Klene, M.;

- Adamo, C.; Cammi, R.; Ochterski, J. W.; Martin, R. L.; Morokuma, K.; Farkas, O.; Foresman, J. B.; Fox, D. J. Gaussian16 Revision C.01. 2016; Gaussian Inc. Wallingford CT.
- (47) Allouche, A.-R. Gabedit A Graphical User Interface for Computational Chemistry Softwares. *J. Comput. Chem.* **2011**, *32*, 174–182.
- (48) Liu, T.; Chen, F. Multiwfn: A Multifunctional Wavefunction Analyzer. *J. Comp. Chem.* **2012**, *33*, 580–592.
- (49) Desfrancois, C. Determination of electron binding energies of ground-state dipole-bound molecular anions. *Phys. Rev. A* **1995**, *51*, 3667.
- (50) Hendricks, J.; de Clercq, H.; Freidhoff, C. B.; Arnold, S. T.; Eaton, J. G.; Fancher, C.; Lyapustina, S. A.; Snodgrass, J. T.; Bowen, K. H. Anion solvation at the microscopic level: Photoelectron spectroscopy of the solvated anion clusters, $\text{NO}-(\text{Y})_n$, where $\text{Y} = \text{Ar}, \text{Kr}, \text{Xe}, \text{N}_2\text{O}, \text{H}_2\text{S}, \text{NH}_3, \text{H}_2\text{O}$, and $\text{C}_2\text{H}_4(\text{OH})_2$. *J. Chem. Phys.* **2002**, *116*, 7926–7938.
- (51) Hendricks, J.; Lyapustina, S. A.; de Clercq, H.; Snodgrass, J.; Bowen, K. Dipole bound, nucleic acid base anions studied via negative ion photoelectron spectroscopy. *J. Chem. Phys.* **1996**, *104*, 7788.
- (52) Brzeski, J.; Jordan, K. Non-valence anions of pyridine and the diazines. *J. Phys. Chem. A* **2022**, *126*, 5310–5313.
- (53) Svozil, D.; Frigato, T.; Havlas, Z.; Jungwirth, P. Ab initio electronic structure of thymine anions. *Phys. Chem. Chem. Phys.* **2005**, *7*, 840–845.
- (54) Gutsev, G. L.; Bartlett, R. J. A theoretical study of the valence- and dipole-bound states of the nitromethane anion. *J. Chem. Phys.* **1996**, *105*, 8785.

- (55) Hao, H.; Shee, J.; Upadhyay, S.; Ataca, C.; Jordan, K. D.; Rubenstein, B. M. Accurate Predictions of Electron Binding Energies of Dipole-Bound Anions via Quantum Monte Carlo Methods. *J. Phys. Chem Lett.* **2018**, *9*, 6185–6190.
- (56) Gulania, S.; Jagau, T.-C.; Sanov, A.; Krylov, A. I. The quest to uncover the nature of benzonitrile anion. *Phs. Chem. Chem. Phys.* **2020**, *22*, 5002.
- (57) Kronik, L.; Stein, T.; Refaely-Abramson, S.; Baer, R. Excitation Gaps of Finite-Sized Systems from Optimally Tuned Range-Separated Hybrid Functionals. *J. Chem. Theory Comput.* **2012**, *8*, 1515–1531.
- (58) Cencek, W.; Szalewicz, K. On asymptotic behavior of density functional theory. *J. Chem. Phys.* **2013**, *139*, 024104.
- (59) Rabilloud, F. Assessment of the Performance of Long-Range-Corrected Density Functionals for Calculating the Absorption Spectra of Silver Clusters. *The Journal of Physical Chemistry A* **2013**, *117*, 4267–4278.
- (60) Zapata, F.; Luppi, E.; Toulouse, J. Linear-response range-separated density-functional theory for atomic photoexcitation and photoionization spectra. *The Journal of Chemical Physics* **2019**, *150*, 234104.
- (61) É.Brémond,; Sancho-García, J.; Pérez-Jiménez, A.; Adamo, C. Double-hybrid functionals from adiabatic-connection:The QIDH model. *J. Chem. Phys.* **2014**, *141*, 031101.
- (62) Kalai, C.; Toulouse, J. A general range-separated double-hybrid density-functional theory. *J. Chem. Phys.* **2018**, *148*, 164105.
- (63) Kalai, C.; Mussard, B.; Toulouse, J. Range-separated double-hybrid density-functional theory with coupled-cluster and random-phase approximations. *J. Chem. Phys.* **2019**, *151*, 074102.

TOC Graphic



How accurately can DFT describe non-valence anions?

Supporting Information

Guillaume Thiam* and Franck Rabilloud*

*Université de Lyon, Université Claude Bernard Lyon 1, CNRS, Institut Lumière Matière,
UMR5306, F-69622 Villeurbanne, France*

E-mail: guillaume.thiam@univ-lyon1.fr; franck.rabilloud@univ-lyon1.fr

Supporting information:

Table SI1: Calculated dipole moment compared to experimental data.

Table SI2: Calculated isotropic polarizability compared to experimental data.

Figure SI1: Structures of the studied molecules.

Figure SI2: Radial distribution function calculated at ω B97x/(2,3,4sp)-aug-cc-pvtz level for acetaldehyde, acetonitrile, pyridazine and thymine.

Figure SI3: Relationship between the electron binding energy (eBE) and the dipole moment of the molecule.

Figure SI4: RDF calculated at the PBEQIDH and ω B97x levels for acetaldehyde, acetone, acetonitrile, FMgF, nitromethane, thymine.

Table SII: Calculated dipole moment, in Debye, compared to experimental data. (Nsp) means aug-cc-pvtz with N additional *s* and *p* functions whose exponents have been determined by multiplying the previous most diffuse exponents by 0.3.

molecule	(0sp)	(1sp)	(2sp)	(3sp)	(4sp)	Expt
Acetaldehyde	2.9232	2.9234	2.9233	2.9233	2.9233	2.75 ^a
Acetone	3.1159	3.1162	3.1129	3.1161	3.1161	2.88 ^a
Acetonitrile	4.0723	4.0714	4.0714	4.0714	4.0714	3.92 ^a
Adenine	2.4265	2.4257	2.4257	2.4257	2.4257	2.5 ^b
Benzonitrile	4.6984	4.6978	4.6977	4.6977	4.6977	4.2 ^b
Butanal	3.0623	3.0624	3.0623	3.0623	3.0623	2.72 ^a
Cyclopentanone	3.2832	3.2833	3.2833	3.2832	3.2832	2.88 ^a
FMgF	0.00	0.00	0.00	0.00	0.00	
NaONa	0.00	0.00	0.00	0.00	0.00	
Nitromethane	3.6332	3.6347	3.6332	3.6347	3.6347	3.46 ^b
Pivaldehyde	3.4973	3.4973	3.4974	3.4973	3.4973	2.66 ^b
Pyridazine	4.2923	4.2916	4.2916	4.2916	4.2916	3.95 ^b
Succinonitrile	5.787	-	-	-	-	5.72 ^c (EA-EOM-CCSD)
Thymine	4.3884	4.3882	4.3881	4.3881	4.3881	4.1 ^b

^a Ref¹ ; ^b Ref² ; ^c Ref³

References

- (1) Hammer, N. I.; Diri, K.; D., K.; Desfrancois, C.; Compton, R. N. Dipole-bound anions of carbonyl, nitrile, and sulfoxide containing molecules. *J. Chem. Phys.* **2003**, *119*, 3650–3660.
- (2) Abdoul-Carime, H.; Desfrancois, C. Electrons weakly bound to molecules by dipolar, quadrupolar or polarization forces. *Eur. Phys. J. D* **1998**, *2*, 149–156.
- (3) Sommerfeld, T.; Dreux, K.; Joshi, R. Excess Electrons Bound to Molecular Systems with a Vanishing Dipole but Large Molecular Quadrupole. *J. Phys. Chem. A* **2014**, *118*, 7320–7329.
- (4) Gussoni, M.; Zerbi, R. R. G. Electronic and relaxation contribution to linear molecular polarizability. An analysis of the experimental values. *J. Mol. Struct.* **1998**, *447*, 163–215.

Table SI2: Calculated isotropic polarizability, in \AA^3 , compared to experimental data.
(Nsp) means aug-cc-pvtz with N additional s and p functions.

molecule	(0sp)	(1sp)	(2sp)	(3sp)	(4sp)	Expt
Acetaldehyde	4.45	4.45	4.45	4.45	4.45	4.6 ^a
Acetone	6.16	6.16	6.16	6.16	6.16	6.4 ^a
Acetonitrile	4.36	4.36	4.37	4.37	4.37	4.44 ^a
Adenine	13.85	13.86	13.86	13.86	13.86	13.2 ^b
Benzonitrile	12.55	12.55	12.55	12.55	12.55	12.5 ^b
Butanal	7.90	7.90	7.90	7.90	7.90	8.2 ^a
Cyclopentanone	8.84	8.84	8.84	8.84	8.84	9.3 ^a
FMgF	2.66	2.66	2.66	2.66	2.66	-
NaONa	11.15	11.15	11.15	11.15	11.15	-
Nitromethane	4.74	4.76	4.76	4.74	4.74	4.80 ^c
Pivaldehyde	10.11	10.11	10.11	10.11	10.11	10.0 ^b
Pyridazine	8.57	8.58	8.58	8.58	8.58	9.8 ^b
Succinonitrile	8.00	-	-	-	-	-
Thymine	11.99	12.00	12.00	12.00	12.00	11.2 ^b

^a Ref¹ ^b Ref² ; ^c Ref⁴

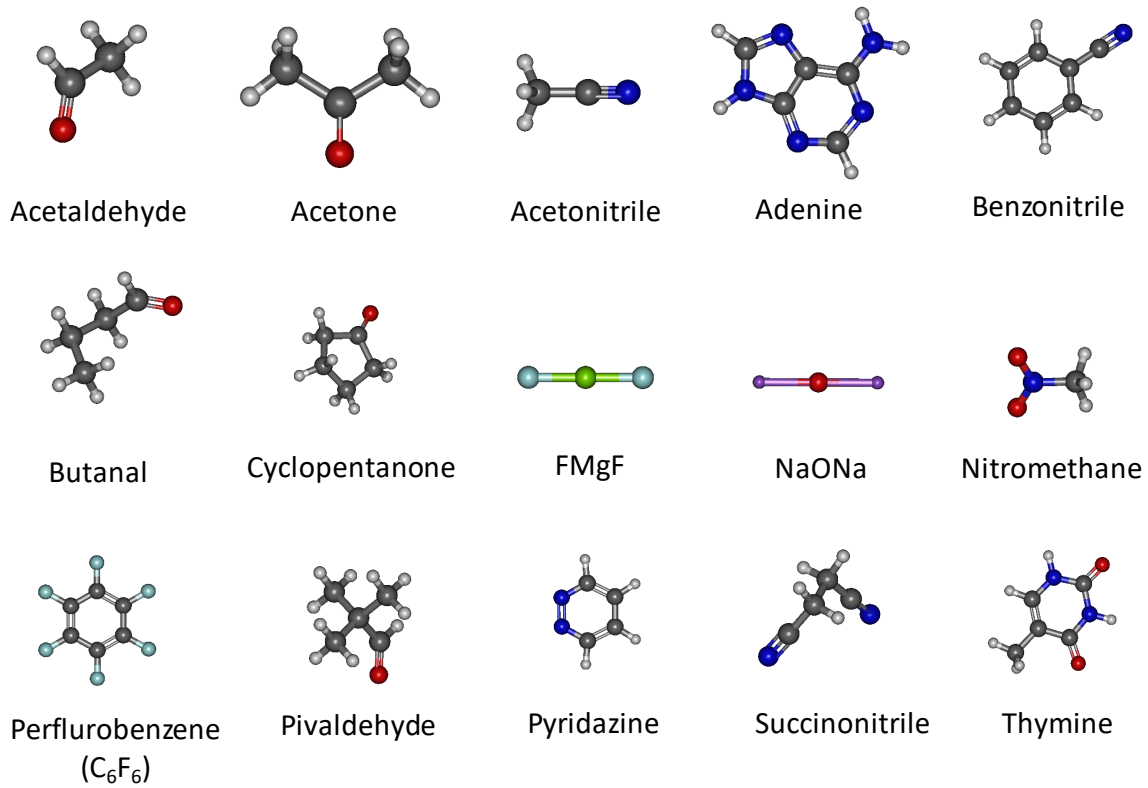


Figure S11: Structures of the studied molecules.

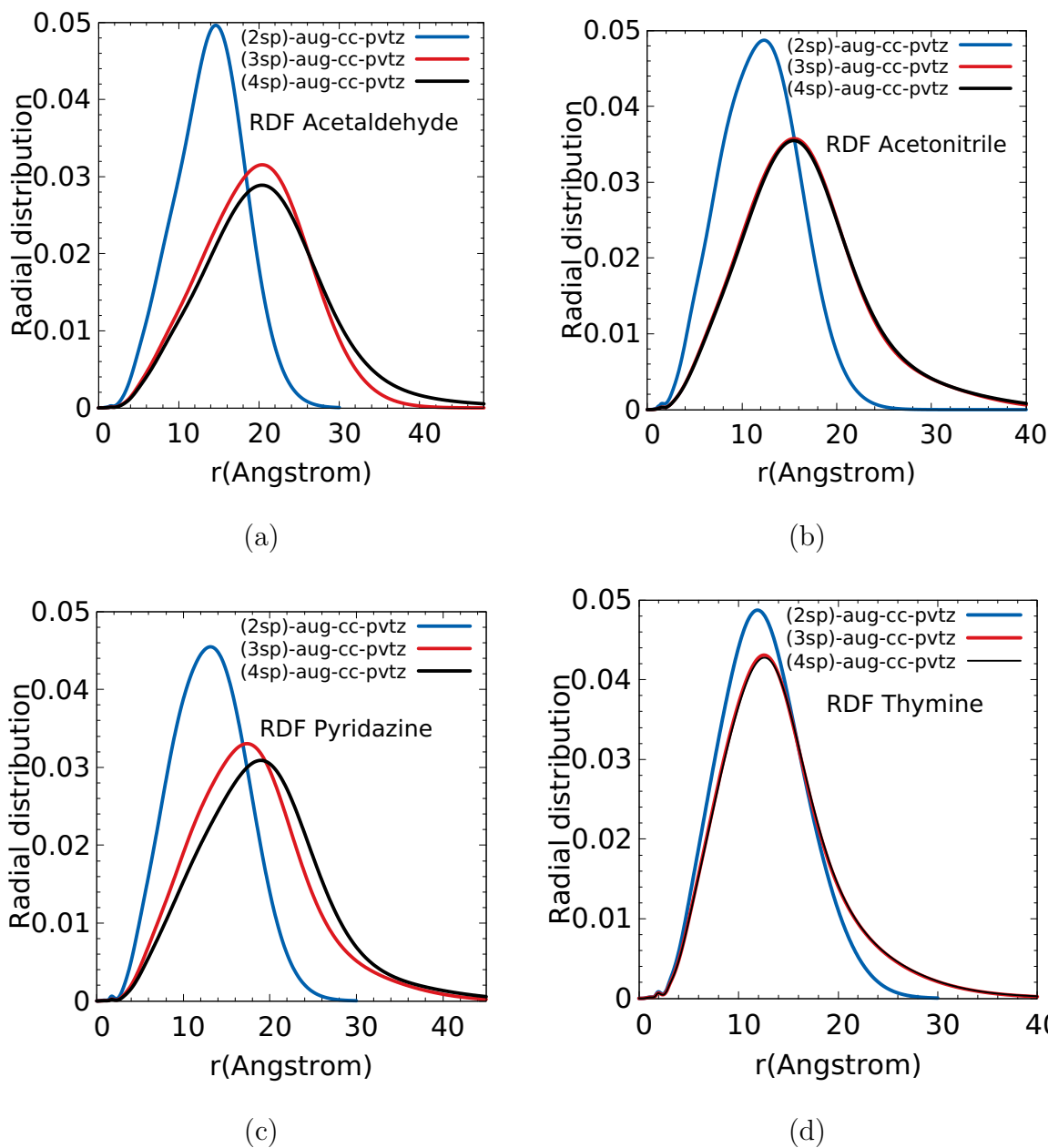
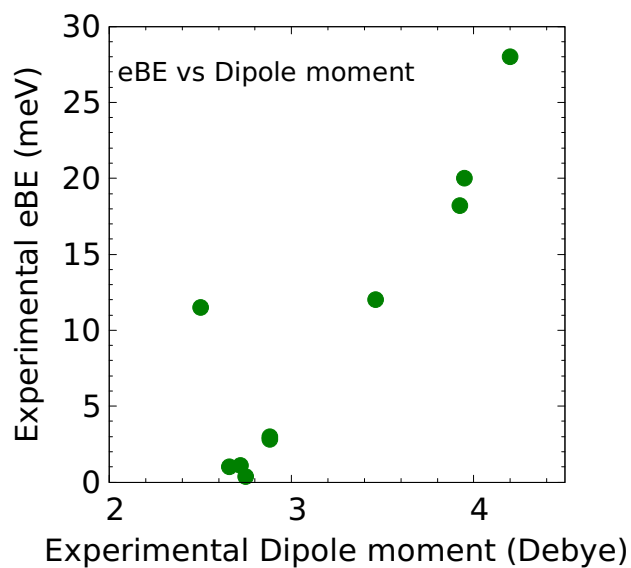
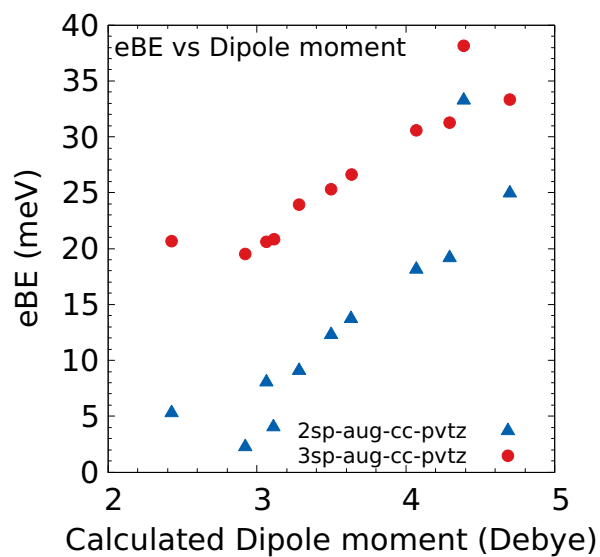


Figure SI2: Radial distribution function calculated at ω B97x/(2,3,4sp)-aug-cc-pvtz level for (a) acetaldehyde, (b) acetonitrile, (c) pyridazine and (d) thymine. For acetonitrile and thymine, the plotted RDF with (3,4)-aug-cc-pvtz basis set are quite similar and exhibit the expected behavior: a diffuse orbital (hill around ~ 12 -20 Angström) corresponding to a bound state.



(a)



(b)

Figure SI3: Relationship between the electron binding energy (eBE) and the dipole moment of the molecule: (a) Experimental values (b) DFT values at ω B97x/(2sp)-aug-cc-pvtz and ω B97x/(3sp)-aug-cc-pvtz levels.

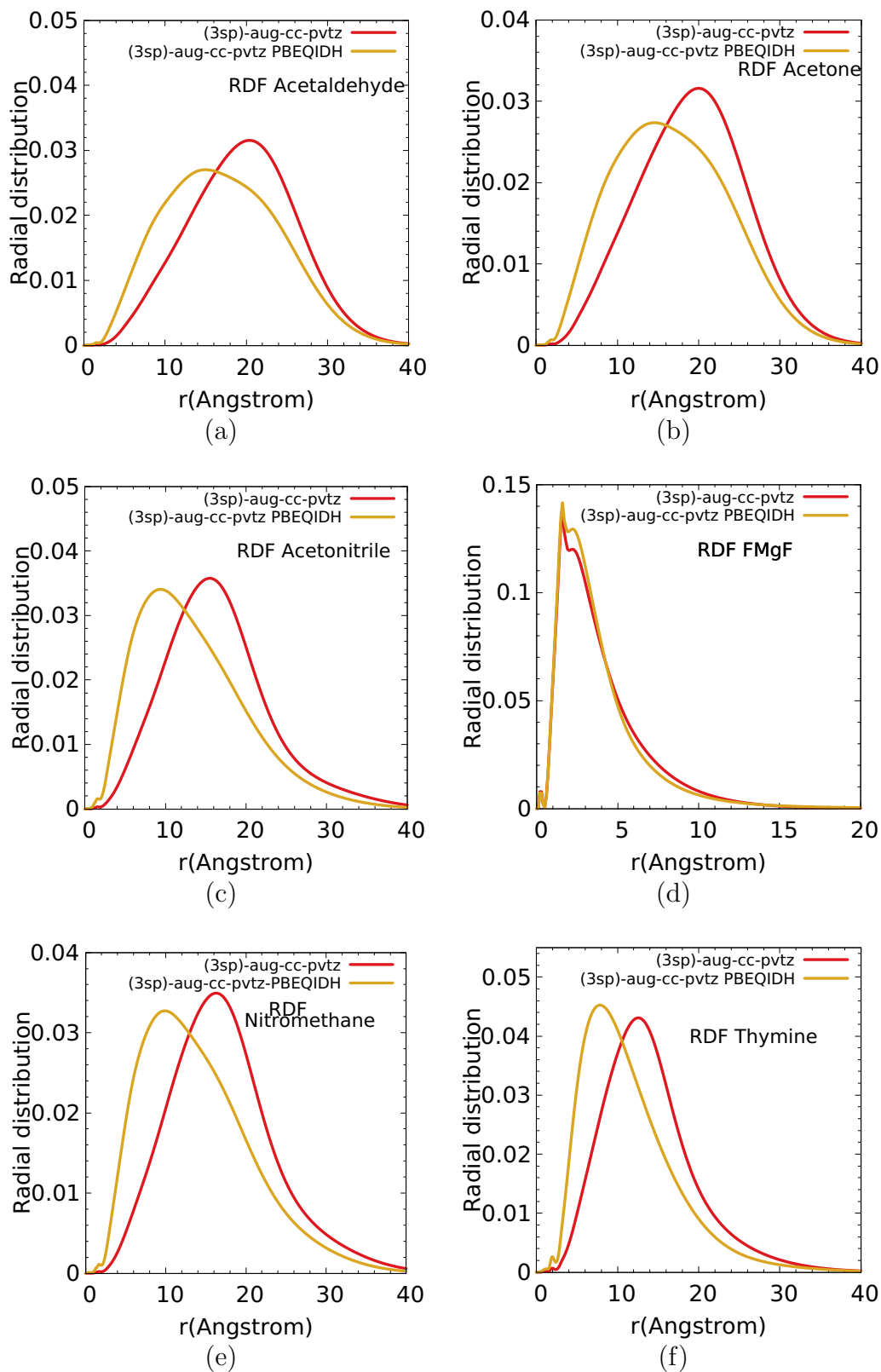


Figure SI4: RDF calculated at the PBEQIDH/(3sp)-aug-cc-pvtz level in gold and at the ω B97x/(3sp)-aug-cc-pvtz level in red for (a) acetaldehyde, (b) acetone, (c) acetonitrile, (d) FMgF, (e) nitromethane, (f) thymine.